

19th ICCRTS
“C2 Agility: Lessons Learned from Research and Operations”

The J-Staff System, Network Synchronisation and Noise

Topics: 2, 5

Alexander Kalloniatis, Mathew Zuparic

POC: A. Kalloniatis

Defence Science & Technology Organisation
Defence Establishment Fairbairn
24 Fairbairn Avenue
Canberra, ACT
Australia

Telephone: +61 2 612 86468

E-Mail: Alexander.Kalloniatis@dsto.defence.gov.au

The J-staff system, Network Synchronisation and Noise

*Alexander Kalloniatis, Mathew Zuparic
Joint & Operations Analysis Division
DSTO
Canberra, Australia*

The Common J Staff System (CJSS) is the means by which military staff headquarters across NATO and the Coalition are structured such that staff internally (to the headquarters) and externally (from another headquarters) are able to implicitly coordinate work. A key challenge of such structures is their tendency to fall into extreme dynamical modes. One is a ‘two-speed’ mode, where units interacting with longer term planning, led by the J5 Planning Branch, fall into a slow cycle of work, while those entities interacting predominately with operations management, led by the J3 Operations Branch, are caught in separate reactive fast cycles. At another extreme is the mode where the reactivity of the J3 overwhelms the whole headquarters, disrupting the ability of the J5 to focus on deliberate planning.

In this paper we examine these dynamics by drawing upon our work on spontaneous synchronisation of phase oscillators on networks, based on the celebrated Kuramoto Model. In particular, we have recently addressed how noise injected into different sub-structures of a general network may disrupt the ability of the network to achieve synchronisation. One of us has previously mapped the Kuramoto Model to the C2 context, by viewing it as a representation of networked linked agents undertaking Boyd’s Observe-Orient-Decide-Act (OODA) loop. We apply this approach to an *ersatz* headquarters to examine the capacity of staff in the J5 Branch to achieve synchronisation with appropriate members of staff in Personnel (J1), Intelligence (J2), Logistics (J4) and Communications (J6) Branches, while also undergoing stochastic interactions with the J3. We explore the range of dynamics under changes in key variables of the model: coupling strengths, the size of noise fluctuations and the degree of inter-Branch links. With validation in specific instances, this model may enable testing the agility of alternate structures, staff numbers and informal (or network centric) linkages.

1. Introduction

In [Kalloniatis 2008, 2012] one of us proposed a new mathematical model for networked Command and Control (C2) systems whose elements are engaged in iterative cycling through continuous Observe-Orient-Decide-Act (OODA) loops [Boyd 1987]. This proposal draws upon the well-known Kuramoto model in the mathematical complex systems literature that displays the phenomenon of “self-synchronisation”. Given the significance of that term in the drive to network-enable military forces through this past decade, its application to Network Centric Warfare (NCW) seemed an obvious thing to undertake; curiously, such an application was missing in the C2 literature until recent years. As some C2 researchers have pointed out, including Boyd [1987], the adversary is often neglected when analysing a C2 system and this was the main motivation in [Kalloniatis 2008, 2012] in adapting the Kuramoto model to the case of two rival C2 systems, which has been termed the ‘Boyd-Kuramoto Model’. In this paper we use the Kuramoto model in a spirit closer to its recent use elsewhere in the C2 community [Dekker 2007, van der Wal 2010, Dekker 2011] for a single system engaged in some aspect of an internal process (choosing from ‘options’ in Dekker and sensor fusion in van der Wal). Specifically, we shall give a proof of concept that the Kuramoto model can be applied to traditionally structured J-staff military headquarters to test whether the different time-frames of planners (J5) and operators (J3) challenge synchronisation within the many supporting branches, such as Personnel (J1), Intelligence (J2), Logistics (J4) and Communications (J6).

The model is expressed as a set of coupled nonlinear differential equations. There already exists a diversity of models of C2. The simplest model for C2 is the wiring diagram. Social Network models enrich this to capture informal interactions. Both are static representations. Business process models, also frequently used for headquarters analysis [Kalloniatis and Wong 2007; Grant 2008], try to incorporate the time dimension but represent ‘tasks’ with little more than resource (personnel, information inputs) and time requirements as attributes. Agent-based distillations offer more sophistication but are often tactically focused and link a rudimentary decision process with kinetic activity in a representation of physical space. In any case, no single model of a complex system, such as the C2 enterprise, has universal validity. The determination of the ‘truth’ of any hypothesis for C2 requires cross-validation between diverse models [Schreiber 2002] across the spectrum of model types [Harré1970]. To that end, the mathematical model expressed in the form of partial differential equations proposed here fills a gap across the spectrum of existing models of headquarters.

To this end, the present model combines a number of elements considered important in C2 in the organisational theory. Boyd’s OODA loop based on his experience of US fighter pilots in the Korean War is now used across the Defence and Business environments as a simple but effective model for the iterative and cognitive aspects of decision-making of individuals and organisations; we mention a former Australian Chief of Joint Operations who spoke of the OODA cycle of his entire headquarters. An OODA cycle takes an amount of time that depends on the intrinsic ability of the individual or unit to internally ‘process’ and the pressures to keep pace with other units (and outpace the adversary, if Red is included as in [Kalloniatis 2008, 2012]). The property of self-synchronisation – that local interactions between networked agents can amplify across a coupled system in order to achieve global effects – has been highlighted with the formulation of NCW; the Kuramoto model is the mathematical representation of this *par excellence*. The Kuramoto model also captures the dimension of ‘coupling’, an organisational property recognised by theorists such as Perrow [1984], Mintzberg [1979] and others of the Contingency Theory School [Donaldson 2001]: connected nodes in a C2 network can have quite different strengths of coupling or degrees of responsiveness to state changes. The model we propose enables an exploration of the balance between ‘dynamism’ (expressed in a frequency spectrum for individual performance of the OODA loop), ‘structure’ (expressed in the network) and ‘coupling’.

In addressing military headquarters designed with the Common J Staff System (CJSS), we meet another phenomenon that can be recast in terms of synchronisation. Recent examples with the United Kingdom's Permanent Joint Headquarters (PJHQ), Australia's Headquarters Joint Operations Command (HQJOC) and New Zealand's Joint Force Headquarters (NZJFHQ) see small or shrinking military establishments mirroring – for reasons of interoperability – within their constraints the structures of the larger USA and NATO. To do this, they have elevated the Planning J5 and Operations J3 Branches with the others providing enabling functions, for example the J15 section feeding Personnel input into planning activities, and the J13 working to the operators. Planning fundamentally should be proactive but potentially sensitive to real-time events, while Operations is unavoidably predominately reactive. This imposes quite different time-scales on the enabling branches, say, the J1 Branch head who must somehow straddle these two time-frames. These pressures continue up to the Commander (J0), which then flow back down to the J5 and J3 themselves challenging their attention, and that of their staff, to their time-frames. It is reasonable then to consider that planners and their enablers need to synchronise to deliver timely plans. We will not get too caught up in whether it is *self*-synchronisation or not: in real headquarters each of hierarchy, formal and informal teams and Chiefs-of-Staff are used so that the network is complex. Synchronisation is also important for operators, who are driven by the 24 hour Battle-Rhythm. However, on the time-scales of a deliberate planning cycle, operator activity can appear quite 'chaotic'. For that reason we apply a further innovation to the Kuramoto model, recently explored theoretically by us [Zuparic, Kalloniatis 2013]: the model subject to noise. In that sense, our focus in this paper is whether synchronisation of OODA cycles can be achieved for planners and their enablers in the time-scales relevant to them *given the stochastic nature of operator OODA cycles*.

Resolving the time pressures can lead to two undesirable extremes. One is that planners and operators decouple and work oblivious of each other, which may be termed a 'two-speed headquarters'. The other is that coupling is so strong that one or the other is driven to the time-frame of the other: planners fail to be proactive, or operators fail to meet the short term requirements of the Battle-Rhythm. This means that *in this context* complete synchronisation is not necessarily 'good behaviour', indeed is inconsistent with C2 agility given its characteristics of flexibility, and responsiveness [NATO 2006]. However, the literature recognises two incomplete forms of synchronisation. 'Partial synchronisation' is where many nodes are locked together while others are subject to random behaviour with respect to the locked core, and 'sub-synchronisation' is where nodes may form into two or three sizeable and internally locked clusters but each cluster moves with its own frequency [Kalloniatis 2010]. Each of these behaviours may be more useful in a C2 context as an indicator of C2 agility. Moreover, elsewhere one of us [Kalloniatis 2010] has shown that sub-synchronisation is consistent with the property of 'emergence' or 'edge-of-chaos'. Our aim nevertheless is to demonstrate the broad value of the model rather than to apply it to a specific situation.

The paper is structured as follows. Section 2 describes the Kuramoto model and the measure of synchronisation, while Section 3 explains the J-staff networks that will be examined in this paper. Section 4 presents some extreme scenarios of two forces respectively in the incoherent and fully self-synchronised states as an aid to understanding of the basic patterns of behaviour. Section 5 explores some sub-synchronised behaviours and demonstrates unexpected behaviours that, in retrospect, can be understood. The paper closes with conclusions and suggestions for future enhancements of the model.

2. The Kuramoto Model

Deterministic Model. The literature on self-synchronisation in mathematically defined cooperative systems is large, going back to Wiener [1961] and Winfree [1967] and scattered across mathematical, physical, biological and computational scientific journals. It was Kuramoto [1984] who succeeded in distilling the bare essentials of such models into the first

order differential equation whose network generalisation we introduce shortly. We use β_i to represent a time-dependent *phase* associated with node i of a complete network of N nodes, $\dot{\beta}_i$ is the angular rotation speed via the derivative of the phase with respect to time t , ω_i represents a ‘natural’ or ‘intrinsic’ frequency, usually randomly chosen from a statistical distribution, and σ is a coupling constant. The role of β_i as a phase is seen when it is reinserted in the complex variable $\chi_i = e^{i\beta_i}$. A general network is represented using the adjacency matrix A_{ij} whose elements take value one if a link (or edge) exists between nodes i and j and are zero otherwise; for simplicity we remain within the bounds of undirected graphs, though further generalisations are possible. The governing time evolution equation is then:

$$\dot{\beta}_i = \omega_i + \sigma \sum_{j=1}^N A_{ij} \sin(\beta_j - \beta_i). \quad (1)$$

The behaviour of the system can be visualised as points moving about the unit circle as in Figure 1. At any point in time each oscillator will be represented by a point on that circle.

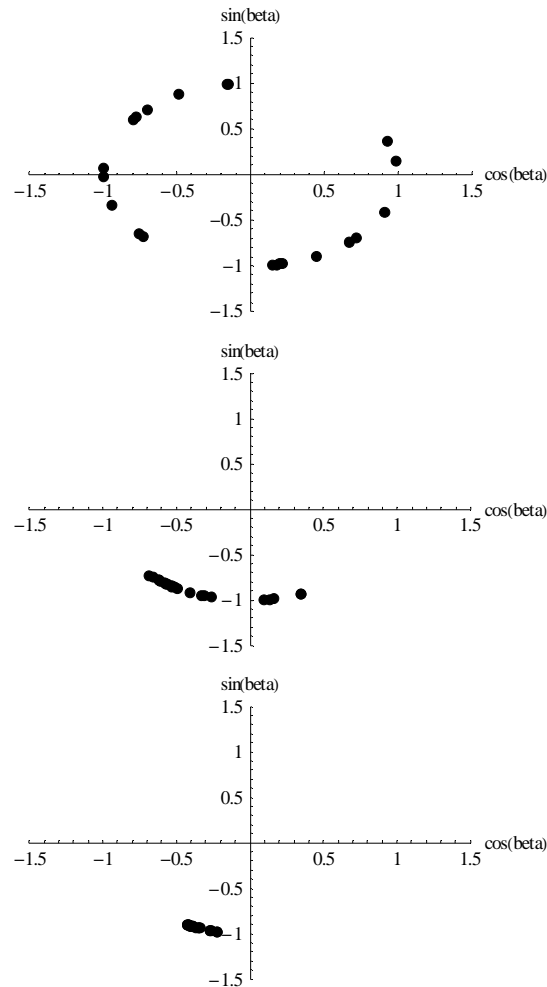


Figure 1 Visualising the individual oscillators as points distributed on the unit circle at a snapshot in time for different values of coupling: weak coupling (top), strong coupling (middle) and very strong coupling (bottom).

For weak coupling the points will be randomly distributed around the circle (Figure 1, top), given the random individual frequencies. For strong coupling the points move with the same

angular speed and group increasingly together as the coupling is increased (Figure 1, middle and bottom). To measure the degree of synchronisation we adopt Kuramoto's order parameter:

$$r = \sum_{j=1}^N e^{i\beta_j} . \quad (2)$$

At strong coupling r converges to one ('complete synchronisation' as in Figure 1, bottom), while at weak coupling it zig-zags around the value zero ('incoherence' Figure 1, top). Special cases of this order parameter can be selected by only summing over specific sets of nodes, for example 'planners' separately from 'operators', which we define, respectively, as r_p and r_o .

Mapping to C2. Translating this to the C2 context, the phase $\beta_i(t)$ represents the point in a continuous decision (or OODA) cycle of agent i at some time t . The network represents the C2 structure itself: the relationships of agents who need to mutually adjust their individual decision cycles. The coupling σ is a somewhat more abstract concept but can be seen as how 'quickly' one agent should adjust their progress through the decision cycle given a change in the progress by any other. The 2π -periodicity of the sine function is appropriate in that it locally synchronises decision cycles within the 'current phase'. The frequency ω_i is how many decision cycles per unit time can be achieved by agent i . This is chosen from a random distribution, representing the underlying heterogeneity between individual decision makers in the C2 system. Training and discipline can narrow that distribution; namely, introducing more homogeneity in the population of decision makers. But the intent is nonetheless to retain some degree of heterogeneity. Moreover, one does not have the luxury of 'managing' that heterogeneity: the C2 system is not designed with individuals of certain frequencies placed deliberately at certain nodes.

Certainly in the NCW literature, such as [Alberts and Hayes 2007] and references therein, the desired self-synchronisation is applied to *activity* in the external environment. I am proposing that the precursor to this is synchronisation of *decision cycles* and therein mapping the phase of the Kuramoto model to the decision cycle; another implementation of the Kuramoto model is possible at the level of activity and is that used in [Dekker 2007, 2011]. These two options are not very far apart: a decision cycle in a context such as a headquarters will very often leave a trail of external artefacts (draft documents, emails, chat or verbal communication) that indicate the stage of OODA of a unit or individual; these artefacts are thus points of reference for another in the same organisation in synchronising their cycle. In other words, even the cognitive stages of Observe-Orient-Decide involve some form of social enterprise, when one steps beyond Boyd's original application to the isolated fighter pilot alone in the cockpit.

Applying Noise. The Kuramoto deterministic system is transformed into a stochastic differential equation (or 'Langevin equation') by adding terms to Eq.(1) that involve functions of time whose values *are not correlated between time instances*. In our case we introduce two forms of noise, additive Γ_a and multiplicative Γ_m , whose values are drawn from a Gaussian distribution of mean zero and unit variance (Gaussian White Noise). The additive noise will be applied to individual nodes as a time-dependent addition to the frequencies ω_i . The multiplicative noise is applied across links between nodes. In full then, the stochastic system takes the form:

$$\dot{\beta}_i = \omega_i + \gamma_a \Gamma_a^a + \sigma \sum_{j=1}^N A_{ij} \sin(\beta_j - \beta_i) + \gamma_m \sum_{j=1}^N R_{ij} \beta_j \Gamma_i^m . \quad (3)$$

The quantities γ_a, γ_m are coupling constants and the matrix R_{ij} is a further adjacency matrix representing the network of interactions across which multiplicative noise is applied.

Noise in C2 systems. Interpreting this noise for the C2 context is different for the additive and multiplicative cases, but at heart both represent the degree to which the human dimension cannot be microscopically tracked and modelled, analogous to the microscopic collisions of suspend colloid particles in the original observation of Brownian motion. Additive noise specifically means there is a random time-dependent element to how fast a cycle is completed: no individual processes information or makes decisions with the same speed in every instance as individual internal factors (such as, for example, mood and health) may vary from instance to instance. (Note that the *external* influences are captured through the network interactions.) Multiplicative noise represents the clarity of the interaction between individual nodes and therefore impacts on the coupling strength. Indeed, because such clarity is obscured in states of heightened activity we apply this term to the operators. Thus we may see the application of multiplicative noise as the onset of a crisis to which the headquarters must respond. As with many real instances of crisis, these are short lived as staff initially scramble to develop a response but then gradually the management of the response folds into a more sustainable steady-state. Thus we will apply noise only for finite periods of time.

Note that, because our focus in this proof of concept model is the synchronisation of planners, we have not built in an interaction for operators that is locally synchronising (such as a sine function): in the absence of noise operators will synchronise only to the degree their Branch heads are synchronised through the planning interactions (in that respect it is genuinely not *self*-synchronisation).

3. The J-staff model

Networks. Formally we work with a headquarters of 19 members: the Commander J0, 6 Branch heads (J1-J6, we ignore here the less universally implemented J7-J9), and individual staff J13, J15 and so on. At the lowest level whole teams may be inserted, but the modelling principle remains the same. This hierarchy is represented in the wiring diagram of Figure 2. Note that in this, and subsequent, diagrams the arrow is only used to order the layers in the construction of the network – it plays no operational role in the mathematical formulation which is always undirected graphs.

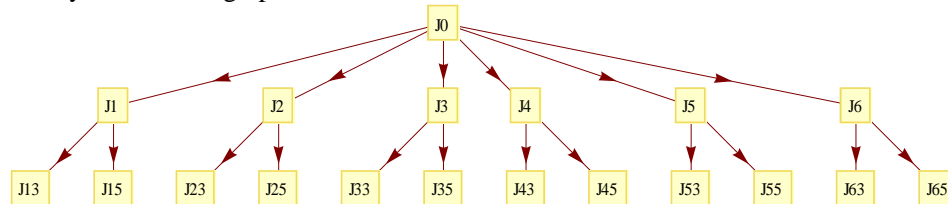


Figure 2 The J-staff hierarchy of the model

This hierarchical representation belies the manner in which this C2 organisation works. In our model planning interactions take place according to the network in Figure 3: the J5 is responsible to the Commander for drawing together the overall operational plan, with the staff work conducted by the J53 subordinate, who in turn draws upon contributions from peers in other branches, the J15, J25, J45, J65. However these junior officers in turn work to their branch heads who in turn report to the Commander. Note that here we exclude the J55 who would work to even longer term, strategic, time-frames to which the operational planning cycle may be subordinate; this requires modelling nested loops which we do not address here.

In military doctrine this staff dynamic is articulated as the Operational Planning Process (OPP) or (in Australia) Military Appreciation Process (MAP), where key logical ‘gates’ such as Mission Analysis and Course of Action Analysis are stepped through. One may see such processes as an elaboration again of the OODA loop. Therefore we shall represent the completion of a cycle of planning as one OODA cycle, and the time for this will be captured as the inverse frequency of the planning nodes to be discussed further below.

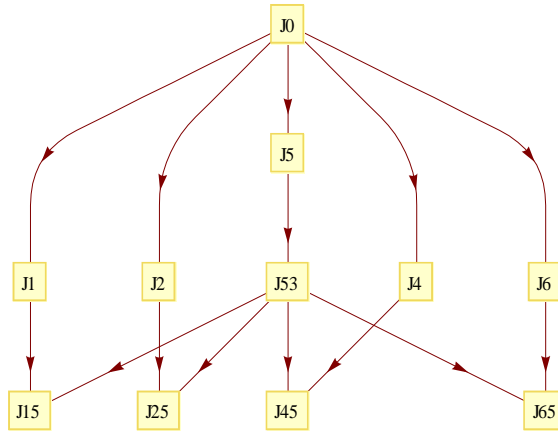


Figure 3 The planning interaction network

Operators interact according to the network in Figure 4. The J33, focused on real time operations, interactions with the J3 who turns to the J35 for rapid planning but reports issues to the Commander. This officer in turn seeks rapid input from the other Branch specialists (J13, J23, J43, J63), who seek guidance from their Branch heads.

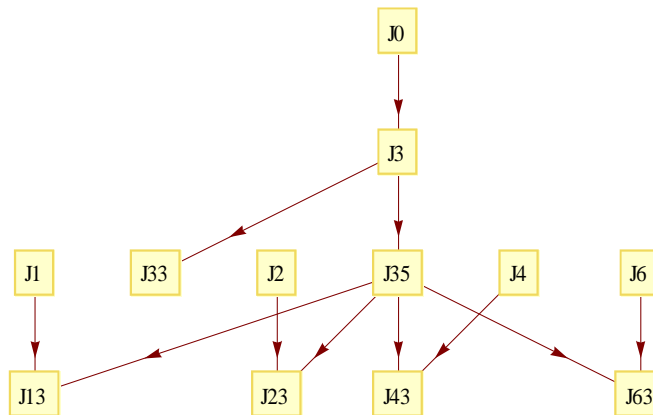


Figure 4 The operations interaction network

This process may be seen as reflecting a Daily Battle-Rhythm but where the Commander prefers to receive a briefing only from the J3. There are many alternatives to this, such as a daily brief with the J3 and J2, or indeed with all Branch heads. All of these are straightforwardly implementable in this model. As has been said many times already, our aim here is to show how any such network may be integrated into a mathematical model of synchronisation and its outputs used to make judgements about the success of that network in C2.

Frequencies. The frequency, or inverse period, reflects the speed through a decision cycle. Unlike the traditional Kuramoto model which draws frequencies from some statistical distribution, here we shall choose quite regular values and put the randomness in the additive noise. We set a time scale by assigning a period of 1 time unit to operators and in turn 15 time units to a planning cycle. Thus, given the daily battle-rhythm, we may see 1 time unit roughly as a day and planners in turn work to a roughly two week planning cycle. The periods are then assigned as shown in Table 1.

Table 1 Periods for a decision cycle

J staff units	Period (time units)
J33	0.5
J0, J1, J2, J3, J4, J6, J13, J23, J35, J43, J63	1
J15, J25, J45, J5, J53, J65	15
J55	30

Note that the J33 real-time operations staff has a much shorter period of 0.5 units and, conversely, the J55 strategic planner a longer period of 30 units. But both of these nodes are quite peripheral to the present model. More significantly, the J5 works to the same intrinsic period as their subordinate J53 in this model. The model could also test what changes if the J5 worked to the same period as the other Branch heads. Frequencies are then the inverse period.

4. Tuning and basic behaviours of the model

We solve Eq.(3) numerically using Mathematica with 10^6 discretisation points. Calculations take between a few seconds to a few minutes (for extreme noise cases, for which there can be memory issues) on a standard desktop Windows XP or 7 workstation. Before applying noise, and with network structure and frequencies fixed, the only free parameter is the coupling σ . We tune this by requiring *that in the absence of noise the planners achieve a stable behaviour* of total synchronisation with $r_p \approx 1$. This is thus consistent with a steady pattern in which planners can be proactive in thinking through a plan. This is achieved at $\sigma = 0.3$. We then *apply noise to the operators* – reflecting their focus on short-time disruptions - (technically, by introducing step functions in the defining Eq.(3)) for finite amounts of time. Indeed, to see the change in behaviour between the onset of additive noise and multiplicative noise we first switch on the additive noise, then the multiplicative noise, which is then sustained for some finite period of time to provide opportunity for the dynamic behaviour to settle down. Then the noises are switched off in reverse order. We equate the noise constants, $\gamma_a = \gamma_m \equiv \gamma$, and examine the behaviours for different values of γ . We show in Figure 5 a typical instance of the dynamical behaviour for a weak value of noise parameter, $\gamma = 0.1$, in terms of plots of the three order parameters, r, r_p, r_o , for the whole headquarters, the planners and the operators respectively, as functions of time. In this case the noise is sufficiently strong to weakly perturb the planners but strongly perturb the operators.

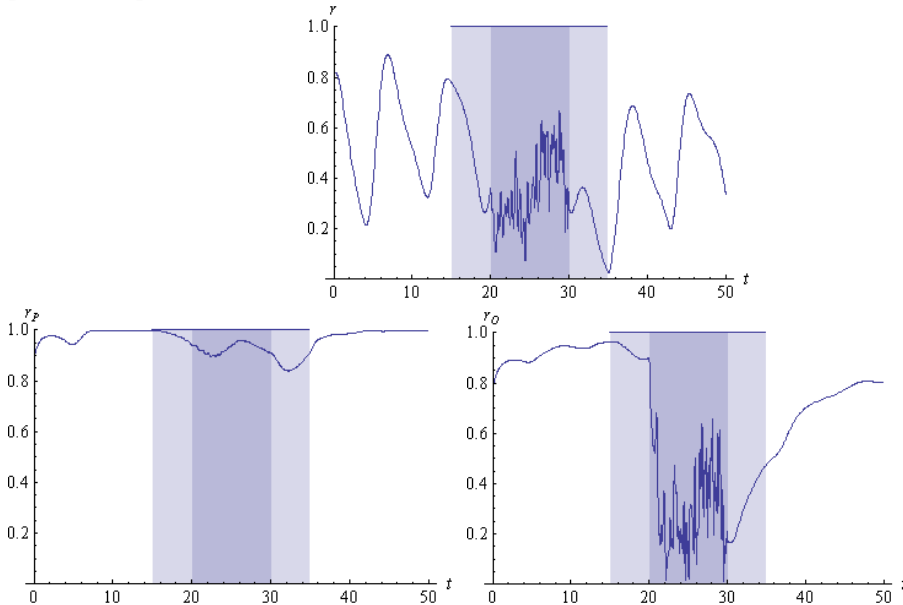


Figure 5 Plots of the three order parameters as functions of time for coupling sufficient to allow planners to synchronise $\sigma = 0.3$ and weak noise $\gamma = 0.1$. In light shaded regions only additive noise is applied while in darker regions both additive and multiplicative noise is applied.

More specifically, we observe that in the absence of noise the overall system shows quite extreme but slow periodic fluctuations in r . We comment on these further as we progress. But these do not change in character with additive noise (light shaded region), but become quite rapid with both forms of noise applied in the dark shaded region (Figure 5, top). As noises are switched off the original behaviour is restored. Contrastingly, the planners, whose order parameter is shown in Figure 5 (bottom, left) synchronise in less than 10 time units which clearly has reached a plateau $r_p = 1$ (as intended by the setting of the coupling constant) by the time additive noise is applied at $t = 15$ (in other words by the time of their second cycle). With the additive noise there is a slight drift which is not seriously exacerbated with the application of multiplicative noise. However, for the operators ((Figure 5, bottom, right) there is also some degree of synchronisation in the absence of noise. This synchronisation is local to them but not synchronised with the planners hence the initial fluctuations in the top part of Figure 5 whose periodicity will be seen to reflect a clustering into two groups. Moreover, because the operators are not subject to the sine interaction in Eq.(3), it is a second order consequence of the coupling of the Branch heads to their planners. The noise, unsurprisingly, completely disrupts this local synchronisation as it is applied directly across their links. Overall we could say that Figure 5 represents a ‘two speed’ headquarters – one part of the staff are barely affected by disruptions to other parts though there are second order effects in play.

At the other extreme, we show the behaviour for relatively strong noise constant $\gamma = 0.9$ in Figure 6. Again, before noise is applied overall there are periodic fluctuations (top) because planners and operators have separately synchronised to a high degree (r_p and r_o close to one respectively in the bottom left and right figures). Up this point it is another instance of the behaviour seen before the noise for weak noise constant. When additive noise is applied (light shaded regions) even the planners are disrupted strongly – in this instance their order parameter zig-zags twice in the time interval. Finally the multiplicative noise strongly disrupts the operators, to whom it is directly applied, but even the planners undergo erratic behaviour with some modulation suggestive of its origin as a second order effect. This is precisely because of the flow: $J33 \rightarrow J3 \rightarrow J0 \rightarrow J5 \rightarrow J53$ and beyond.

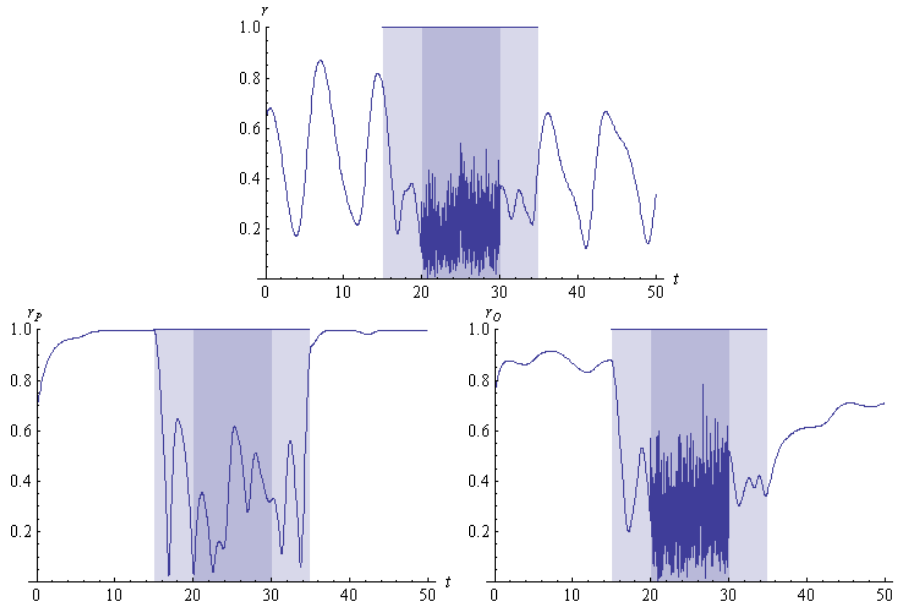


Figure 6 Plots of the three order parameters as functions of time for coupling sufficient to allow planners to synchronise $\sigma = 0.3$ and strong noise $\gamma = 0.9$. In light shaded regions only additive noise is applied while in darker regions both additive and multiplicative noise is applied

5. Analytic Behaviour and Mean First Passage Time

There is value in understanding analytically, where possible, some aspects of the dynamics. The case of multiplicative noise is beyond our powers presently, however we can understand at a deeper level the behaviour arising from the additive noise on the operators. We achieve this by examining the equations in the vicinity of a fixed point for phase synchronisation where some approximations of the non-linear equations can be made. Then the stability, namely exponential decay of fluctuations back to the fixed point, or instability, namely exponential divergence of fluctuations, can be analysed.

Specifically, we consider the connected network of planners at the instant additive noise is switched on. As we have seen, we have chosen the coupling constant such that the system always reaches phase synchronisation without the noise. In this setting the planners phases obey the fixed point relationship $\beta_i \approx \beta_j$, which allows us to approximate the sine interaction by its leading linear behaviour. This allows us to express the interaction term as

$$\sum_{j=1}^{N_p} A_{ij} \sin(\beta_j - \beta_i) \approx -\sum_{j=1}^{N_p} L_{ij} \beta_j ,$$

where N_p is the number of planners and we have introduced the graph *Laplacian* matrix, $L_{ij} = D_{ij} - A_{ij}$. The eigenvalues and eigenvectors of the Laplacian are particularly useful for understanding dynamical systems on a network [Bollobás 1998]. For example, the eigenvalues, denoted λ_s , $s = (0, 1, \dots, N_p - 1)$, are zero or positive $0 = \lambda_0 \leq \lambda_1 \leq \dots \leq \lambda_{N_p-1}$; the number of zero eigenvalues in fact corresponds to the number of disconnected components a network breaks up into. For the planners network the spectrum of eigenvalues is shown in Figure 7, showing the one zero value (the planners network does not have disconnected components) and a number of degenerate values which reveal symmetries in the planners network.

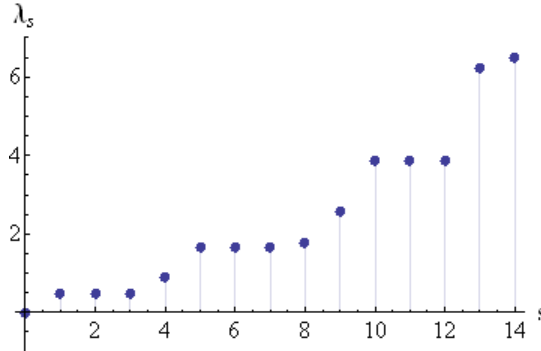


Figure 7 Plots of the eigenvalues of the planners Laplacian

The relevant dynamical equations for the planning network at the instant the additive noise is switched on is

$$\dot{\beta}_i \approx \omega_i + \gamma_a \Gamma_i^a - \sigma \sum_{j=1}^{N_p} L_{ij} \beta_j . \quad (4)$$

The orthonormal eigenvectors of the Laplacian, denoted $\vec{v}^{(s)}$, allow the system to be diagonalised and solved. The phase angles for the planners are expanded into Laplacian ‘eigenmodes’

$$\beta_i(t) = \sum_{s=0}^{N_p-1} x_s(t) v_i^{(s)} . \quad (5)$$

We then project all the terms in Eq.(4) onto the s-th eigenvector, for example for the noise:

$$\Gamma_i^a(t) = \sum_{s=0}^{N_p-1} \Gamma_s(t) \nu_i^{(s)}. \quad (6)$$

(Such a linear combination of independent uncorrelated Gaussian white noise gives similarly uncorrelated Gaussian white noise.) A similar equation defines the frequency projected vector $\omega^{(s)}$. Applying Eq.(5,6) to Eq.(4), we obtain the decoupled system of linear ('Langevin') equations for the eigenmodes, where for the moment we make

$$\dot{x}_s = \omega^{(s)} + \gamma_a \Gamma_s - \sigma \lambda_s x_s. \quad (7)$$

Let us now pause and consider the above sets of equations before ploughing ahead analytically. If we consider the above equations in the absence of noise, then each eigenmode has the solution of exponential decay in time with decay constant $\sigma \lambda_s > 0$ due to the positive semi-definiteness of the eigenvalues. This is consistent with the Kuramoto model showing Lyapunov stability about the phase synchronised fixed point. Each eigenmode decays to a non-zero constant $x_s(t \rightarrow \infty) = \omega^{(s)} / (\sigma \lambda_s)$. Thus it is assured that the sine approximation we applied at the start of this section is valid. In terms of the planners, *small fluctuations in their cycle are damped and they always relax to their natural planning rhythm.*

Consider now the system with noise. It is generally known that in systems with additive noise (applied here via the operator nodes) eventually a sequence of fluctuations will arise in the random distributions that will be sufficient to knock the system out of the basin of attraction of the fixed point [Schuss 2010]. This will apply no less to Eq.(7). This does not mean that the overall system (Eq.(3)) will be unstable, but it does mean that at some point in time we expect the linear approximations of the sine function used to arrive at Eq.(4) to no longer hold, and one has to consider the full non-linear system which may restabilise the behaviour. *The planners are continually disrupted and there is a time after application of the noise in which their natural relaxation to their routine cycle can no longer occur.*

The Mean First Passage Time (MFPT), denoted by $E[\tau]$, now enables a probabilistic characterisation of this time to instability, *or mean (over many instances of noise) time in which the planners are driven outside of the basin of attraction of the fixed point of their natural cycle.* Formally, the MFPT is the expected time the process in Eq.(7) will cross a designated boundary such as that for a basin of attraction of a fixed point. In this instance, we choose the boundary which leads to the sine approximation to break down. In general, it is quite hard to derive exact bounds on the eigenmodes x_s which lead to the phase difference $\beta_i - \beta_j$ being sufficiently far apart as to break the sine approximation (see Appendix A of [Zuparic and Kalloniatis 2013]). However, in our experiences with systems of 20-30 nodes [Kalloniatis 2010; Zuparic and Kalloniatis 2013] a sufficient "heuristic" boundary is given simply by $x_s = \pm 1$.

With the boundaries chosen, the MFPT is calculated through solving the *Andronov-Vitt-Pontryagin equation* [Schuss 2010], given in the Appendix. From Figures 5 and 6, we know that the processes in Eq.(7) have reached steady state by the time the additive noise is switched on. Hence the initial values are simply the steady state values of the deterministic process $x_s = \omega^{(s)} / (\sigma \lambda_s)$. Using this fact about the initial values x_s of the MFPT, we can compute a closed form solution, which is given in the Appendix. It turns out that it is convenient to view the MFPT as a function of two combinations of the various parameters of the model: $\mu = \omega^{(s)} / \sigma \lambda_s$, $\chi = \sigma \lambda_s / \gamma_a^2$. (We suppress the subscript 'a' in γ_a for the remainder of this section.) Plotting the MFPT in terms of these parameters we arrive at a surface shown in Figure 8. In this plot we indicate as large dots points coinciding with parameter choices of interest, for some of which we have numerically solved the full system of equations. In

particular, they correspond to the two lowest non-zero eigenvalues of the planners graph Laplacian, for which $\omega^{(s)}/(\sigma\lambda_s) < 1$, meaning that these are the modes ‘closest’ to instability.

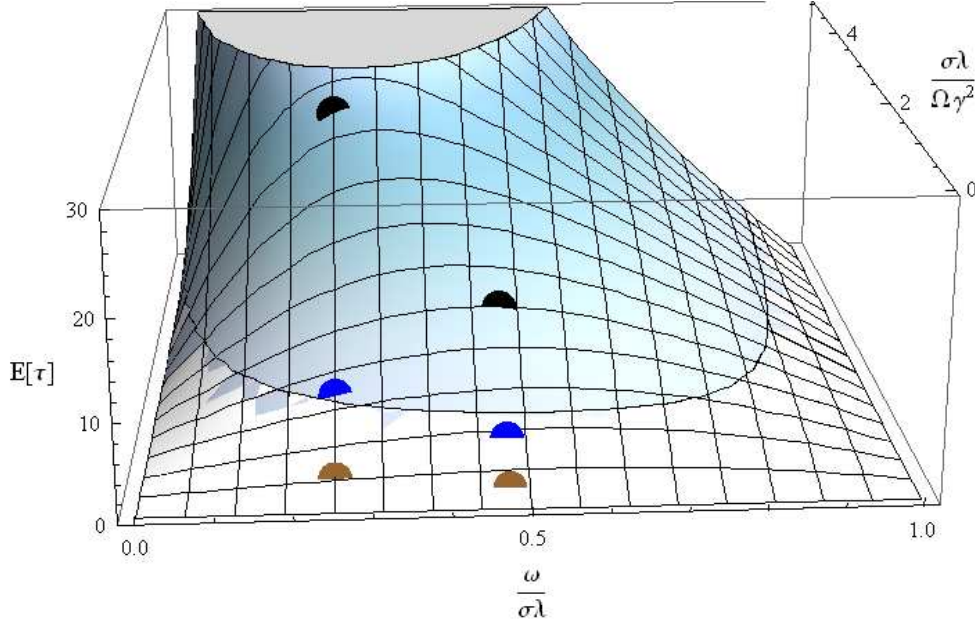


Figure 8 Plot of the MFPT for the parameters μ and χ with the frequency ω set to $1/15$ as a function of frequency to coupling ratio (x-axis, left-to-right) and coupling to noise strength ratio (y-axis, into the page). The surface is divided into two regions, white and blue, with the dividing line between the two regions being the line of equi-MFPT (with $E[\tau] = 5$). The dots on the surface are the MFPTs for specific parameter choices and graph topology for the planners network. The two brown dots are the MFPT for $\gamma = 0.9$ and $\lambda = 0.89$ (left brown dot)/ $\lambda = 0.47$ (right brown dot). The two blue dots are the MFPT for $\gamma = 0.5$ and $\lambda = 0.89$ (left blue dot)/ $\lambda = 0.47$ (right blue dot). Finally, the two black dots are the MFPT for $\gamma = 0.3$ and $\lambda = 0.89$ (left black dot)/ $\lambda = 0.47$ (right black dot).

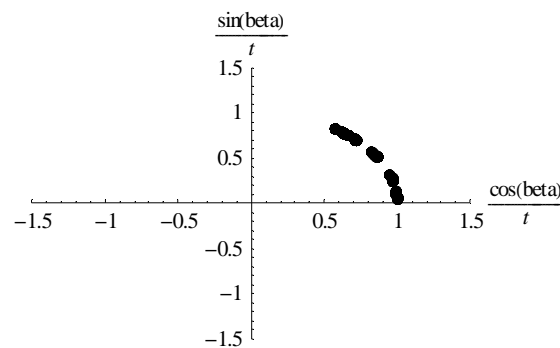
To orient ourselves with this figure it is worth appreciating that infinite MFPT means an infinite amount of time is required for the first passage of the system across the boundary. This may be termed absolute stability in the presence of noise. However, apart from this special point, *if noise is sustained for long enough eventually stability will be lost*. So there is only relative stability and the question becomes how long can noise be sustained on average before the system is driven from its equilibrium point. Thus the rising peak in Figure 8 is the region of higher relative stability. Towards the edges, with small values of MFPT, are regions of contrastingly high instability. We have introduced a plane in the plot to show points of equal MFPT at $E[\tau] = 5$, the time at which multiplicative noise is switched on in our numerical solutions of the system. Thus the two black points, for the two lowest eigenvalues of the Laplacian, but at the lower value of noise constant $\gamma = 0.3$ show high values of MFPT. So, small noise means relative stability. In fact, for the even weaker values of noise of $\gamma = 0.1$ for which we solved the equations the MFPT is many orders of magnitude larger and off the scale of this plot. This is consistent with the weak response of the system to the noise seen in Figure 5. Contrastingly, the two brown points, again for the two lowest eigenvalues, at noise constant $\gamma = 0.9$ lie in regions of small MFPT in Figure 8. So, increasing noise increases the instability. Again, this is consistent with the severe disruption the noise causes in Figure 6. In between we show the blue points which lie on the boundary for the time at which multiplicative noise is applied. We may describe this as a region of intermediate stability. But this value of noise strength leads to further interesting behaviours once multiplicative noise is applied.

In summary, the planes of equi-MFPT in Fig.8 allow *estimation of the average time for which planners with specific coupling and frequencies (x-axis) can tolerate noise of specific strength (y-axis) propagated through the operators before driven completely from their natural cycle.*

6. Emergence

Emergence is often described as the property of dynamical systems to ‘surprise’ – to exhibit unexpected behaviours. Formally, we adopt Laughlin’s [2005] definition of emergence as: system qualities or behaviours that are not reducible to the system components but arise from their interactions. In this case there are a number of layers in the headquarters design of our model: 1) the individual planner and operator oscillators at the nodes of the networks 2) the two networks as entities unto themselves, and 3) the collective headquarters system. I shall be primarily interested in emergence across these layers; namely, behaviours that are not reducible to one of these three layers.

Emergence in dynamical systems is also associated with an intermediate region between order and disorder, stability and instability or the ‘Edge of Chaos’. Above we have already discussed the role of fixed points for the space of oscillator states. Edge of Chaos sees trajectories neither exponentially converging back to the point (Lyapunov stable) nor diverging away (Lyapunov unstable) but following power-law dependence on time. Mixed in with more standard stable and unstable directions, this gives rise to forms of patterned behaviour through collective degrees of freedom. Our colleague Richard Taylor has shown that there are thresholds for more types of stable fixed points in the equal frequency Kuramoto model than just ‘globally phase synchronised’ [Taylor 2012]. In the Kuramoto model with non-equal frequencies, one of us has also identified such fixed points [Kalloniatis 2010]: for many classes of networks there is an intermediate range of coupling where nodes have formed a small number (two to three) of clusters, within which oscillators are locked to a common frequency, but across which there remains incoherence; a further increase in coupling tips these clusters into forming a single overall cluster. Technically, these behaviours occur in a regime of non-vanishing imaginary parts of Lyapunov exponents but vanishing real parts of Lyapunov exponents – giving stable limit cycles and the formal Edge of Chaos characterisation. Thus a system of many oscillators with random frequencies *may* devolve to a two or three body system of effective modes, the internally locked clusters, sufficient to give rise to structured behaviour, depending on the vagaries of how the frequencies and connections are distributed: oscillators with nearly identical frequencies placed at adjacent nodes will tend to cluster. This clustering as an intermediate regime is illustrated in a series of parametric plots for three different values of the coupling σ in Figure 9 for such a system.



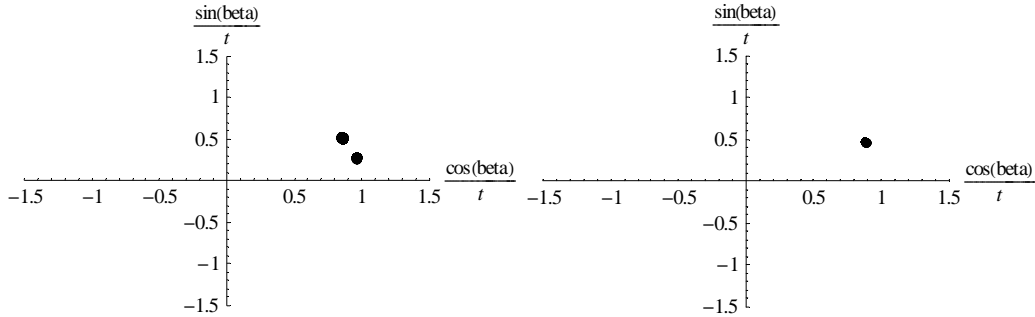
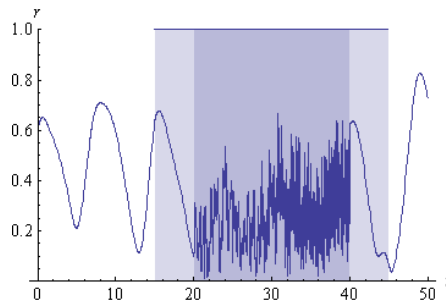


Figure 9 Parametric plots of phase angles over the time duration of cosine and sine of phases divided by time for weak (top), intermediate (bottom left), and strong (bottom right) coupling; respectively these show incoherence (top), intermediate clustering (bottom left) and complete phase locking (bottom right).

Unlike Figure 1, which represents a snapshot in time, we now plot as a series of points the cosine and sine of the phase of an oscillator *for each moment in time*. For any single point one would obtain a circular track. Dividing the cosine/sine *by the time* brings this track, for zero coupling, to a single point consistent with the motion of an individual oscillator about the unit circle being largely uniform in time. Plotting this for all oscillators, for zero coupling, gives a distribution of points lying on the circle (Figure 9, top); unlike the first case in Figure 1, the points here are not spread over the entire circle because dividing by the time here exposes the individual oscillator frequencies (which for the above case are drawn from a distribution between $[0,1]$). Now, as coupling strength increases there is a transition from the multiple points to one single point, corresponding to all oscillators locked to the same phase moving with the average frequency (Figure 9, bottom right). In between these extremes is a state of two independent clusters (Figure 9, bottom left). This intermediate level clustering gives rise to *cyclic* behaviour of the order parameter r . This explains in more depth why, at coupling value $\sigma = 0.3$ *in the absence of noise* the overall order parameter shows cyclic behaviour in the top plots of Figure 5 and Figure 6: planners and operators have formed their own clusters, as alluded earlier.

Can such behaviour occur for our headquarters model in the presence of noise? Indeed it can, and shows up in many instances at $\gamma = 0.5$, which led to the intermediate MFPT region in Figure 8. We plot one example in Figure 10 where three periodically spaced peaks in the order parameter r_p occur through the application of noise in the dark shaded region of Figure 10 (bottom, left). We have generated many of these and sometimes two cycles occur and sometimes four, infrequently more chaotic or even quiescent appear according to the specific instance of the noise.



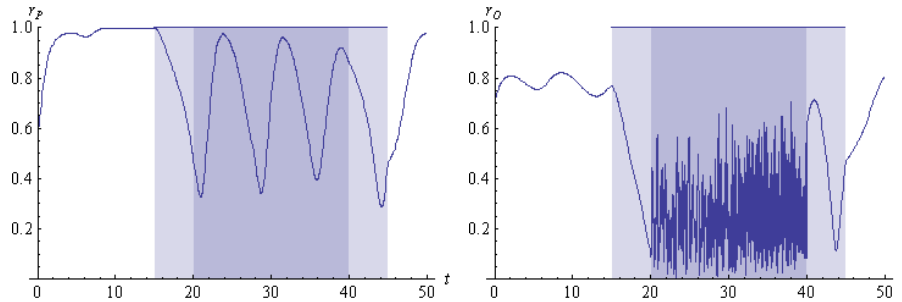


Figure 10 Plots of the three order parameters as functions of time for coupling sufficient to allow planners to synchronise $\sigma = 0.3$ and strong noise $\gamma = 0.5$. In light shaded regions only additive noise is applied while in darker regions both additive and multiplicative noise is applied

Studying individual cases more carefully suggests that this ‘accidental’ herding of planners does not coincide with any natural convergence of their immediate superiors. If anything, in Figure 11, which compares the positions of the planners’ cycles with that of their immediate superiors at the time at which r_p reaches one of its periodic maxima, there is evidence of an *anti-correlation*. In that sense the military hierarchy is playing a double role at this intermediate noise constant value: it is the path for the noise to disrupt the planners in the first place but it indirectly generates a phase shifted convergence of those same planners.

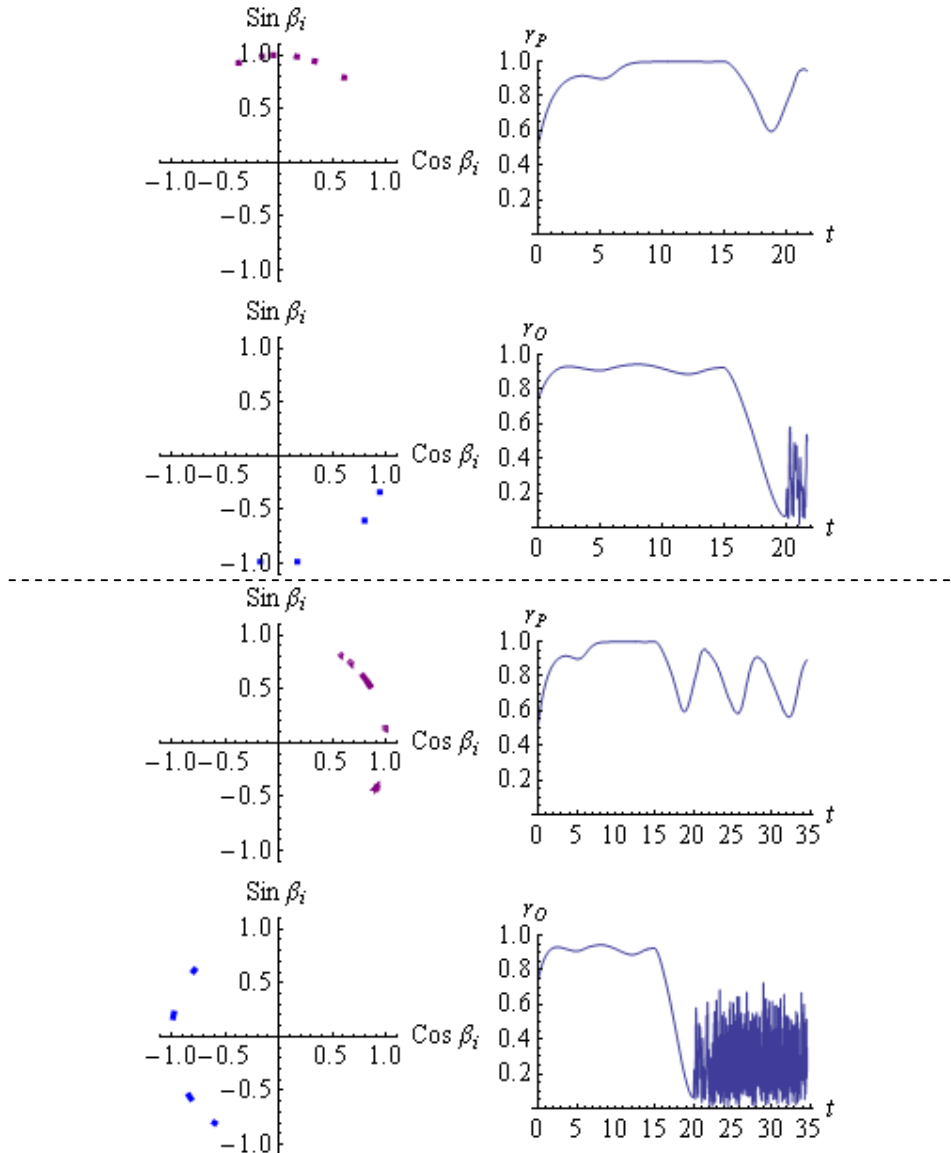


Figure 11 Two quad charts showing snapshots of the positions of planners' J15, J25, J45, J53, J65 cycle (top left of each set of four) and that of their immediate superiors J1, J2, J4, J6 (bottom left) at the time at which the planners order parameter (top right) is close to its peak at the latest time in the right hand plots. Note that the relatively well converged planners are half a cycle shifted with respect to their (less converged) superiors.

7. Conclusions and Future Work

Our aim in this paper was to give a proof of concept that the mathematical formulation of the Kuramoto model provides a basis for representing the structure and dynamics of a military staff headquarters. The basis for this representation is the common feature in both of network structure, and cyclicity in the elementary processes of individuals and their units. Drawing on our recent research of the influence of noise on phase synchronisation we were able to further enrich the model by showing how the unavoidably chaotic, reactive life of operators can flow across to planners who seek to work to tighter planning cycles. Solving the equations numerically we demonstrated basic behaviours of the model that may be recognised in a poorly functioning headquarters: planners who have become so reactive there is no semblance of order to their processes, or so oblivious to the reactivity of their operator colleagues they

are unresponsive to the external environment. However, we were able to show there is an intermediate regime of behaviour where order and chaos are finely balanced, so that the planners achieve regular periods of near synchronisation. We argue this is the regime of an *agile organisation*, where it is able to achieve an ordered behaviour that is *responsive* to the circumstances of fluctuations and interactions. Each instance of this order will be different according to the specific nature of the noise. We have provided some evidence that the hierarchy plays a non-intuitive role in this order. Indeed, the network combines both the peer-to-peer and hierarchical aspects which, we argue, are necessary for both agility and accountability. Further research into the coincidences of structure and frequency can provide insight into how such order can be achieved systematically.

Beyond the particular formulation of this model, there are further refinements of this Kuramoto-like instantiation of a headquarters model. For example, here we have not provided interactions that give the operators scope for locally synchronising, nor, for that matter, the J33 or J55 ('strategic planners'). This is because we lack a formulation for synchronisation within nested loops. Within this spirit, there is scope for representing that each unit in a headquarters may play a different role in an overall *headquarters OODA loop* while nevertheless undertaking their own local (and nested) decision cycle. For example, the J2 predominately enables the Observe and Orient phases with respect to the Red force, the Commander and Branch Heads play a role in the Decide phase, and deployed units in the Act phase. These are elements we anticipate developing in the near future.

Acknowledgements

We are grateful for many discussions with our colleagues with more detailed experience in such real headquarters, especially David Graham, Elizabeth Kohn and Timothy Neville.

Appendix: Laplacian eigenvectors and Mean First Passage Time

In the main body we defined the Laplacian and gave some properties of its eigenvalues. The orthonormal Laplacian eigenvectors, $\vec{v}^{(s)}$, satisfy

$$\sum_{j=1}^{N_p} L_{ij} v_j^{(s)} = \lambda_s v_i^{(s)}, \quad \sum_{i=1}^{N_p} v_i^{(s)} v_i^{(q)} = \delta_{sq}. \quad (8)$$

These vectors also reveal aspects of the underlying graph structure. For example, for the planners Laplacian the two lowest eigenvectors $\vec{v}^{(0)}$ and $\vec{v}^{(1)}$ are shown in Figure 12. Observe that for the zero eigenvector all nodes participate in the vector with value $1/\sqrt{N_p}$ while that eigenvector for the first non-zero eigenvalues picks out certain nodes non-uniformly. In fact these expose the nodes most susceptible to become disconnected with minimal link removals.

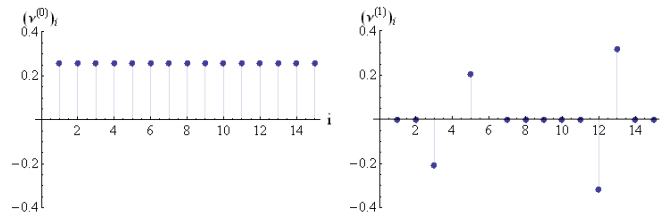


Figure 12 Plots of the eigenvector component values for the normalised “zeroeth” (left) and “first” (right) eigenvectors of the planners Laplacian.

With the boundaries $x_s = \pm 1$, the MFPT is a solution to the *Andronov-Vitt-Pontryagin equation* [Schuss 2010], given for this instance by,

$$\frac{\gamma_a^2}{2} \frac{d^2}{dx_s^2} E_s[\tau] + (\omega^{(s)} - \sigma \lambda_s x_s) \frac{d}{dx_s} E_s[\tau] = -1, \quad (9)$$

with the boundary conditions $E_s[\tau]_{x=1} = E_s[\tau]_{x=-1} = 0$. Reiterating, the MFPT is the expected time taken for the stochastic process in Eq.(7) to hit the boundary given that the process begins in the domain $-1 \leq x_s \leq 1$. The boundary conditions simply state that a process which begins on the boundary takes zero time to cross it. From Figures 5 and 6, we know that the processes in Eq.(8) have reached steady state by the time the additive noise is switched on. Hence the initial values are simply the steady state values of the deterministic process, $x_s = \omega^{(s)} / (\sigma \lambda_s)$. Using this fact about the initial values x_s of the MFPT, the closed form solution of Eq.(9) is given by (see Appendix C of [Zuparic and Kalloniatis 2013]),

$$E_s[\tau] = \frac{\mu \chi}{\omega^{(s)}} \left\{ \operatorname{erfi}(\sqrt{\chi}(1+\mu)) \frac{(1-\mu)^2 H(\chi(1-\mu)^2) - (1+\mu)^2 H(\chi(1+\mu)^2)}{\operatorname{erfi}(\sqrt{\chi}(1+\mu)) + \operatorname{erfi}(\sqrt{\chi}(1-\mu))} + (1+\mu)^2 H(\chi(1+\mu)^2) \right\}, \quad (10)$$

where erfi is the imaginary error function and H is the generalised hypergeometric function:

$$H(x) = {}_2F_2\left(1, 1; \frac{3}{2}, 2 \mid x\right).$$

References

- D.S. Alberts, R.E. Hayes, “Planning: Complex Endeavours”, CCRP, April 2007.
- I. Ali, Coexistence or Operational Necessity: the role of formally structured organisation and informal networks during deployments, 16th ICCRTS, 2011.
- B. Bollobás, “Modern Graph Theory”, Springer, New York, 1998.
- J.R. Boyd, “Organic design for Command and Control”, 1987.
- J.R. Boyd, “The Essence of Winning and Losing”, see the set preserved by Chester Richards, <http://www.danford.net/boyd/essence.htm>.
- L. Chen, J. Lu, Cluster Synchronization in a Complex Dynamical Network with Two Nonidentical Clusters, *Jrl Syst Sci & Complexity*, 21, 20-33, 2008.
- A. Dekker, Studying Organisational Topology with simple computational models, *Jour. Artificial. Societies And Social Simulation*, 10, 2007; <http://jasss.soc.surrey.ac.uk/10/4/6.html>
- A. Dekker, Analyzing C2 Structures and Self-Synchronization with Simple Computational Models, *Proceedings of the 16th International Command and Control Research and Technology Symposium*. Quebec City, Canada, June 21–23, 2011; www.dodccrp.org/events/16th_icrts_2011/papers/055.pdf
- L. Donaldson, “The Contingency Theory of Organizations”, London: Sage Publications, 2001.
- T. Grant, P. Essens, R. Van der Kleij, Reducing Operational Planning Cycle Time using BPR and Concurrent Engineering, 13th ICCRTS, Seattle, 2008.
- R. Harré, “The Principles of Scientific Thinking”, Macmillan, London, 1970.
- W.P. Hughes Jr. (Ret.USN CAPT), “Fleet Tactics and Coastal Combat”, 2nd Edition, Naval Institute Press, 2000.
- A. Kalloniatis, P. Wong, Application of Business Process Modelling to Military Organisations, *Proceedings of SimTechT07*, 2007
- A. Kalloniatis, A new paradigm for dynamical modelling of networked C2 processes, 13th ICCRTS, 2008.
- A. Kalloniatis, From incoherence to synchronicity in the network Kuramoto model, *Physical Review E* 82, 066202, 2010.
- Y. Kuramoto, “Chemical Oscillations, Waves, and Turbulence”, Springer, Berlin 1984.
- R.B. Laughlin, “A different universe: reinventing physics from the bottom down”, Basic Books, 2005.
- H. Mintzberg, “The Structuring of Organizations: A Synthesis of the Research”, Englewood Cliffs, NJ: Prentice Hall, 1979.
- NATO 2006, Exploring new command and control concepts and capabilities, SAS-050 Final Report, January 2006
- C. Perrow, “Normal Accidents: Living with High-Risk Technology”, New York: Basic Books, 1984.

Schreiber, D. 2002. Validating agent-based models: From metaphysics to applications. Annual Conference of the Midwestern Political Science Association, Chicago, IL: April 2002.

Z. Schuss, "Theory and Applications of Stochastic Processes", in: Series in Applied Mathematical Sciences, vol. 170, Springer, New York, 2010.

S.H. Strogatz, From Kuramoto to Crawford: exploring the onset of synchronization in populations of coupled oscillators, *Physica D* 143, 1, 2000.

R. Taylor, There is no non-zero stable fixed point for dense networks in the homogeneous Kuramoto model, *J.Phys.A: Math Theor*, 45 055102, 2012.

N. Wiener, "Cybernetics", 2nd Edition, MIT press, Cambridge, MA, 1961.

A.T. Winfree, *J. Theoret. Biol.* **16**, 15, 1967.

A. van der Wal, Phase Synchronisation of an ensemble of weakly coupled oscillators: A paradigm of sensor fusion, 15th ICCRTS, 2010

M. Zuparic, A. Kalloniatis, Stochastic (in)stability of synchronisation of oscillators on networks, *Physica D* 255, 35–51, 2013.